Supporting Information

García-Fandiño and Sansom 10.1073/pnas.1119326109

SI Text

SI Methods Parametrization was based on that used in previous studies (1): Carbon atoms were modeled as uncharged Lennard–Jones particles with $\sigma cc = 3.400$ Å and $\epsilon cc = 0.086$ kcal mol^{-1}, corresponding to sp2 carbons in the AMBER99 force field. Carbon–carbon bond lengths of 1.4 Å and bond angles of 120° were maintained by harmonic potentials with spring constants of 938 kcal mol^{-1} Å^{-2} and 126 kcal mol^{-1} rad^{-2}, respectively. In addition, a weak dihedral angle potential was applied to bonded carbon atoms. The carbon-water Lennard–Jones parameters were $\sigma co = 3.2751$ Å and $\epsilon co = 0.114333$ kcal mol^{-1}. The parameters for the functional groups COO^- and $NH_3{}^+$ were obtained from the corresponding residues in the Amber force field, Glu and Lys, respectively. The partial charges were modified to C(0.01360)-C (0.80540)-O(-0.9095) in the carboxylate group and C(-0.01430)-N(-0.3867)-H(0.457) in the amine group.

We used the water (SPC/E)/ion combination parameters published by Joung and Cheatham (2) implemented in AMBER10 to prevent crystallization previously reported at high concentrations with other parameter sets (3). The GAFF force field was used for dioleoyl phosphatidyl choline lipids, employed also in previous studies (4) from which we obtained a preequilibrated membrane for subsequent replication. The bilayer was replicated three times in x and y directions [or only twice in the case of the potential of mean force (PMF) calculations], and after carbon nanotube (CNT) insertion, the complete system was solvated. Water in the hydrophobic region of the tails and also inside of the CNT was removed, so that in the first step of the simulation the channel was completely dry. The resultant system was ionized using different salt concentrations (NaCl 1 M, KCl 1 M, and $CaCl_2$ 0.5 M). The initial size of the unit cell was equal to $18.2 \times 17.4 \times 7.0$ nm^3 and contained 560 lipids and approximately 18,000 water molecules.

The equilibrium simulations were performed with the GROMACS 4.0 (5) molecular dynamics program. All the systems were partially optimized, thermalized, and equilibrated, followed by unrestrained simulations for at least 30 ns (time step of 2 fs) for each one of the systems studied. The constant pressure and temperature canonical ensemble was employed with the pressure of 1 bar controlled using a semiisotropic Parrinello–Rahmanbarostat (6), and the temperature of 300 K imposed by a Berendsen (7) thermostat. The LINCS (8) algorithm was employed to remove the bond vibrations. The Particle Mesh Ewald method (9) coupled to periodic boundary conditions was used to treat the long-range electrostatics using a direct-space cutoff of 1.0 nm and a grid spacing of 0.12 nm. Van der Waals interactions were computed using periodic boundary conditions coupled to a spherical cutoff of 1.0 nm.

Poisson–Boltzmann calculations were carried out using the software package APBS (10). These calculations were performed as described in ref. 11. The program HOLE (12) yielded the radius profile of the CNT system and also provided sample points along the pore axis at which to place the ion. The test ions were assigned a Born radius of 0.1680 nm (for Na^+), 0.2172 nm (for K^+), 0.1862 nm (for Ca^{2+}), and 0.1937 nm (for Cl^-) (13). The electrostatic binding energy of the ion was calculated at subsequent positions z as

$$\Delta G_B(z) = G_{pore+ion}(z) - G_{ion} - G_{pore}. \quad \textbf{[S1]}$$

The temperature was 300 K and the dielectric constant ϵp of the pore was set to four, the ionic strength 0.15 M, and the dielectric constant for the solvent was 78.5. For each data point, the ion was placed at a sample point on the pore center line as identified by HOLE. The sample points were 0.25 Å apart along the z axis. The channel was contained in a coarse grid of dimensions 15.1 nm × 15.2 nm × 6.7 nm^3 and 289 points along the z axis were used.

1. Hummer G, Rasaiah JC, Noworyta JP (2001) Water conduction through the hydrophobic channel of a carbon nanotube. *Nature* 414:188–190.
2. Joung IS, Cheatham TE (2008) Determination of alkali and halide monovalent ion parameters for use in explicitly solvated biomolecular simulations. *J Phys Chem B* 112:9020–9041.
3. Case DA, et al. (2008) AMBER 10 (University of California, San Francisco).
4. Siu SWI, Vacha R, Jungwirth P, Böckmann RA (2008) Biomolecular simulations of membranes: Physical properties from different force fields. *J Chem Phys* 128:125103.
5. Hess B, Kutzner C, van der Spoel D, Lindahl E (2008) Gromacs 4: Algorithms for highly efficient load-balanced, and scalable molecular simulation. *J Chem Theory Comput* 4:435–447.
6. Parrinello M, Rahman A (1981) Polymorphic transitions in single crystals: A new molecular dynamics method. *J Appl Phys* 52:7182–7190.
7. Berendsen HJC, Postma JPM, van Gunsteren WF, DiNola A, Haak JR (1984) Molecular dynamics with coupling to an external bath. *J Chem Phys* 81:3684–3690.
8. Hess B, Bekker H, Berendsen HJC, Fraaije JGEM (1997) LINCS: A linear constraint solver for molecular simulations. *J Comput Chem* 18:1463–1472.
9. Essman U, et al. (1995) A smooth particle mesh Ewald method. *J Chem Phys* 103:8577.
10. Baker NA, Sept D, Joseph S, Holst MJ, McCammon JA (2001) Electrostatics of nanosystems: Application to microtubules and the ribosome. *Proc Natl Acad Sci USA* 98:10037–10041.
11. Beckstein O, Tai K, Sansom MSP (2004) Not ions alone: Barriers to ion permeation in nanopores and channels. *J Am Chem Soc* 126:14964–14965.
12. Smart OS, et al. (1996) Hole: A program for the analysis of the pore dimensions of ion channel structural models. *J Mol Graphics* 14:354–360.
13. Rashin AA, Honig B (1985) Reevaluation of the Born model of ion hydration. *J Chem Phys* 89:5588–5593.

	NaCl 1M	KCl 1M	$CaCl_2$ 0.5M
Pristine	*Data in Fig. 2 (Main article)*	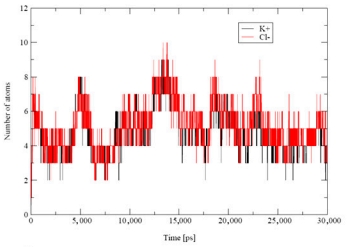	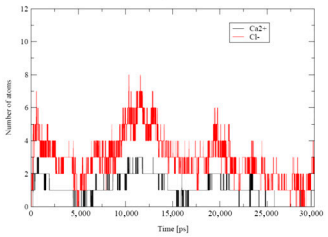
C-2	*Data in Fig. 2 (Main article)*	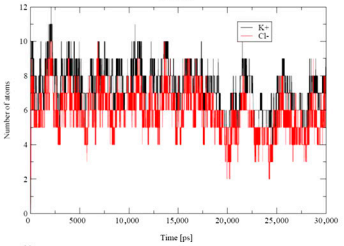	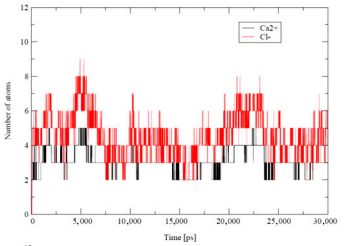
C-4	*Data in Fig. 2 (Main article)*	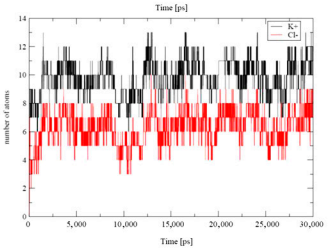	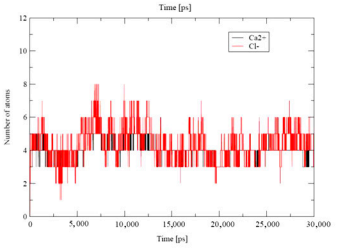
C0	*Data in Fig. 2 (Main article)*	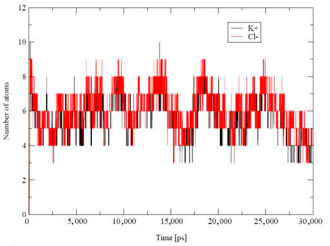	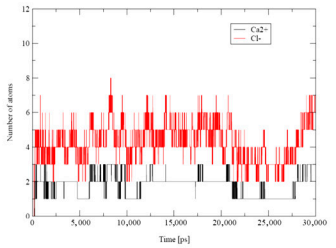
C-1	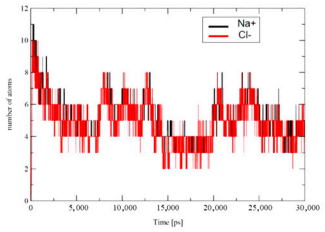	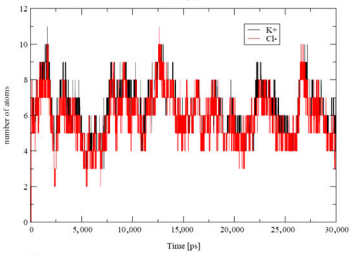	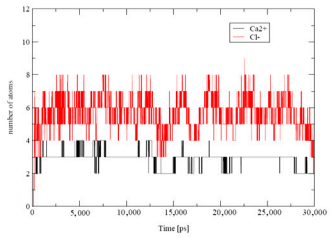
E-2	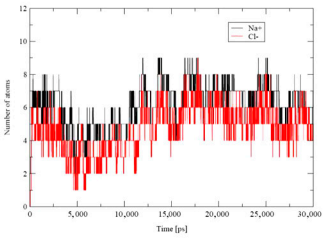	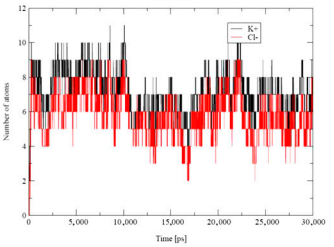	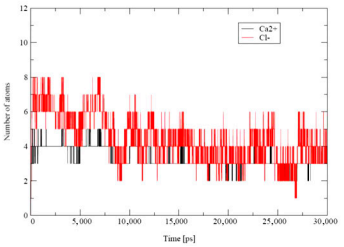

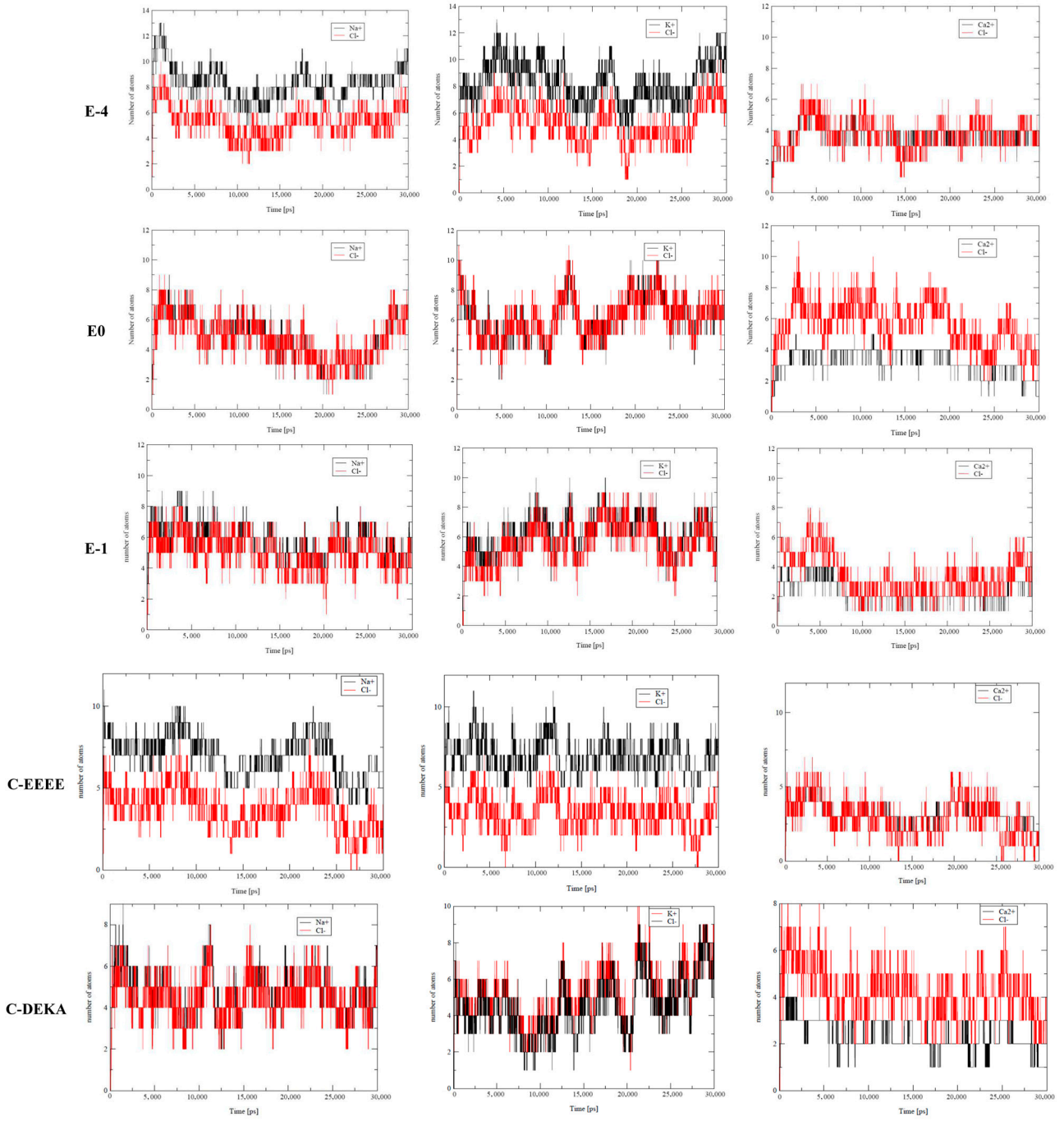

Fig. S1. Numbers of cations and chloride ions inside the nanopores during equilibrium molecular dynamics simulations.

	NaCl 1M	KCl 1M	$CaCl_2$ 0.5M
Pristine	*Data in Fig. 3 (Main article)*	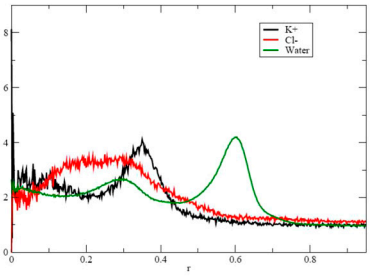	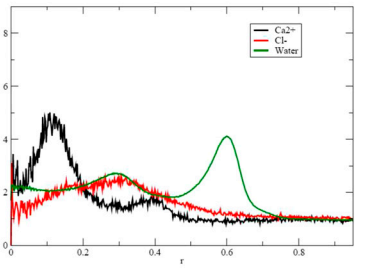
C-2	*Data in Fig. 3 (Main article)*	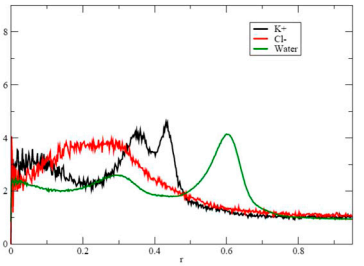	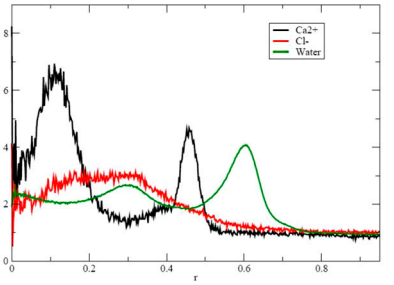
C-4	*Data in Fig. 3 (Main article)*	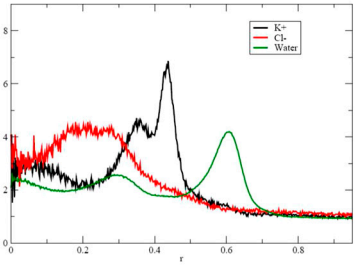	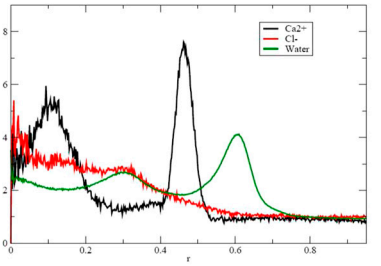
C0	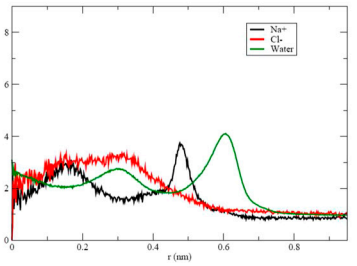	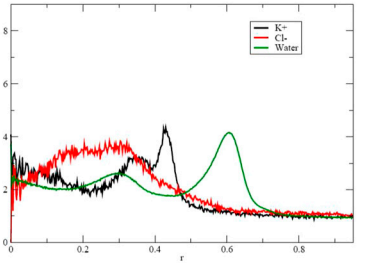	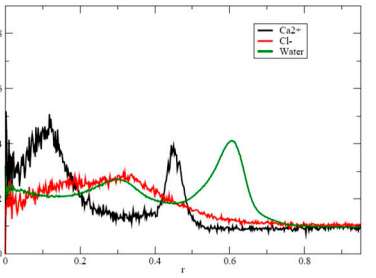
C-1	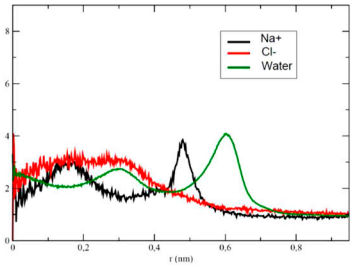	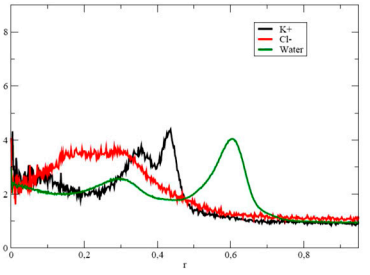	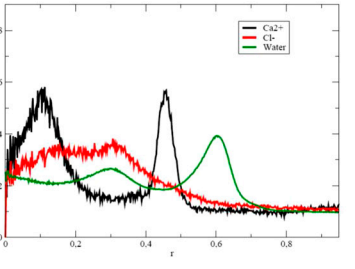

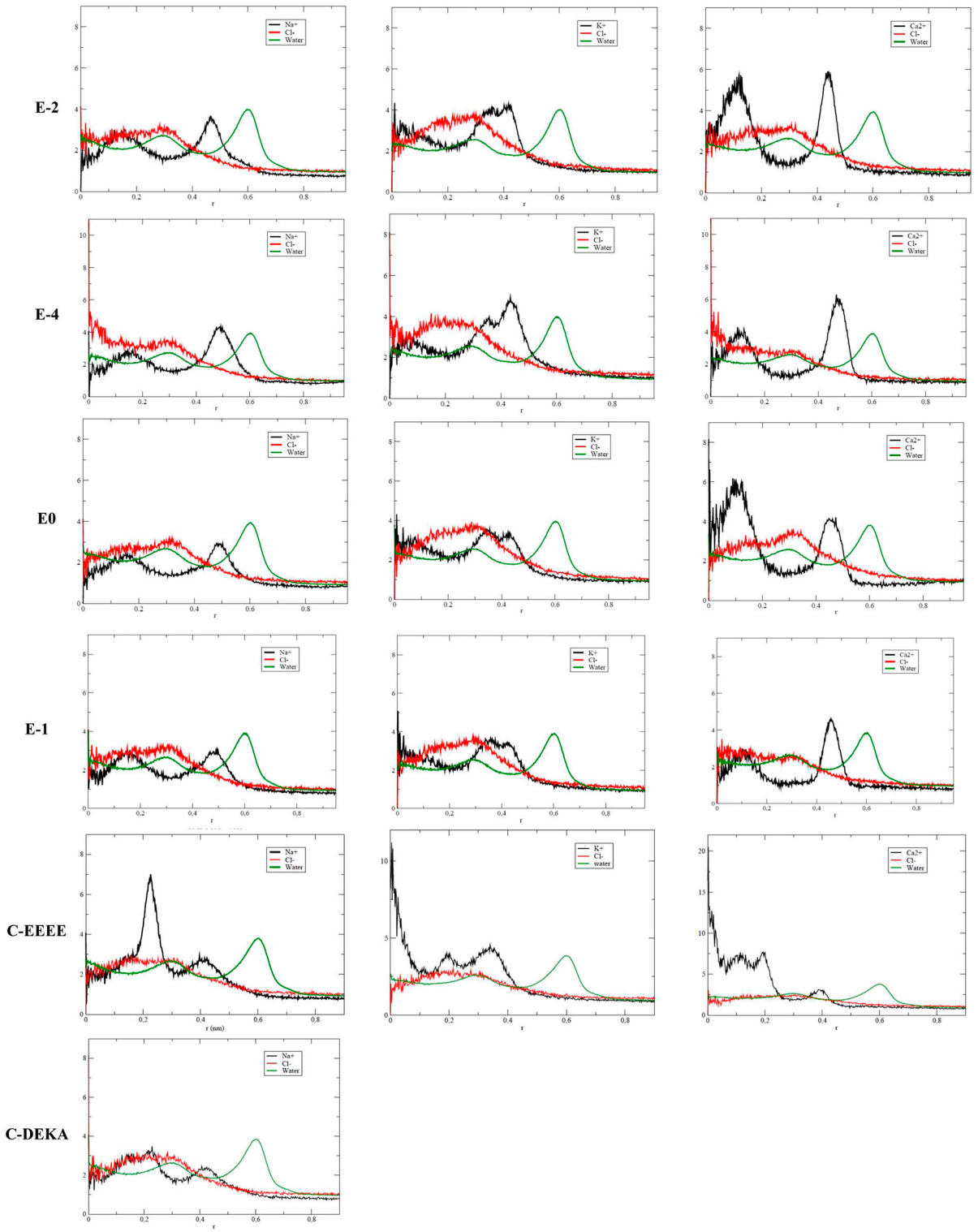

Fig. S2. Radial distributions of cations (black), Cl- ions (red), and water (green).

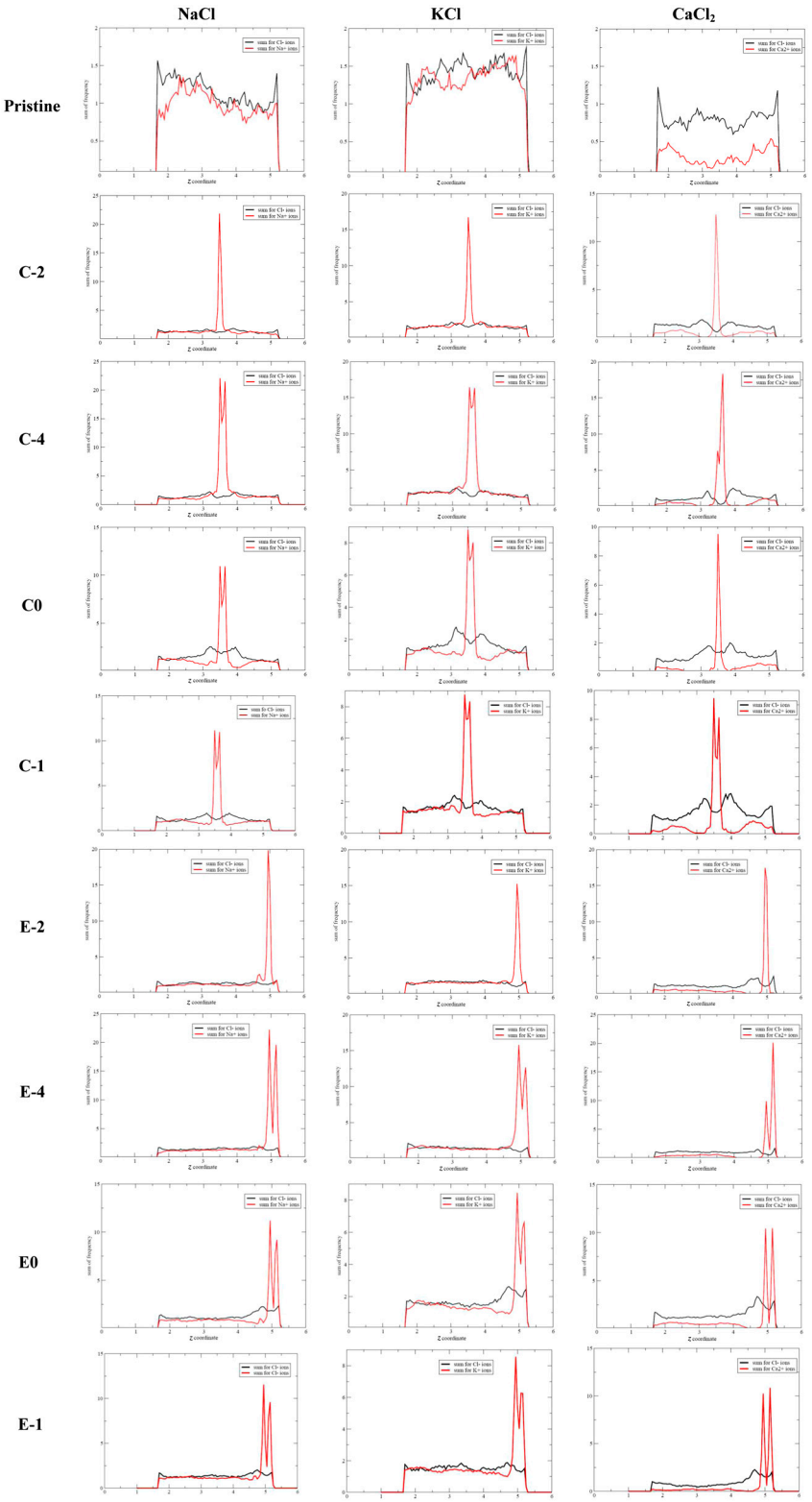

Fig. S3. Distributions of cations (red) and Cl^- ions (black) along the long axis (*z*) of the nanopores. The selectivity filters are positioned at *z ca.* 0 nm.

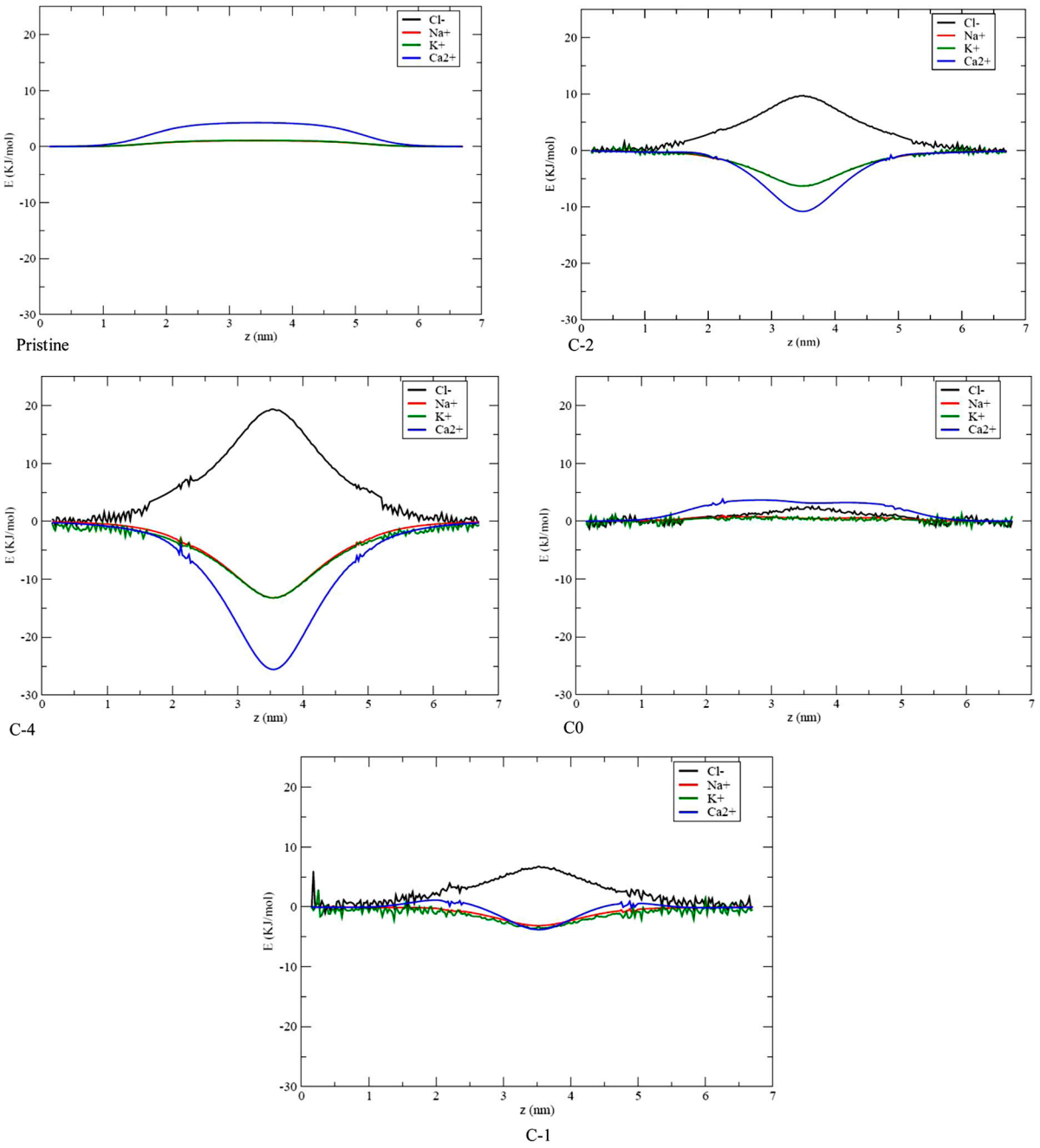

Fig. S4. Poisson–Boltzmann profiles for several ions for the pristine CNT (*A*) and those derivatized with 2 COO- C-2 (*B*), 4 COO- C-4 (*C*) 2 COO- plus 2 NH_3^+ C0 (*D*), and 2COO- plus NH_3^+/CH_3 C-1 groups at the central position of the pore.

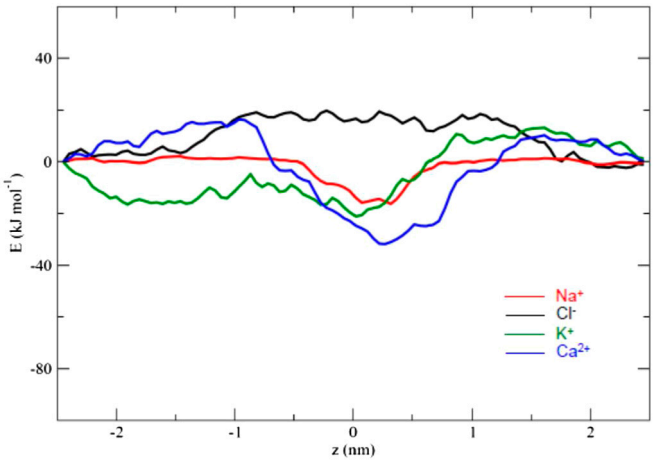

Fig. S5. PMFs for single ions as a function of position along the *z* axis of the pore of C-1. The bilayer extends from *z ca.* −1.5 to +1.5 nm. The selectivity filters are positioned at *z ca.* 0 nm.

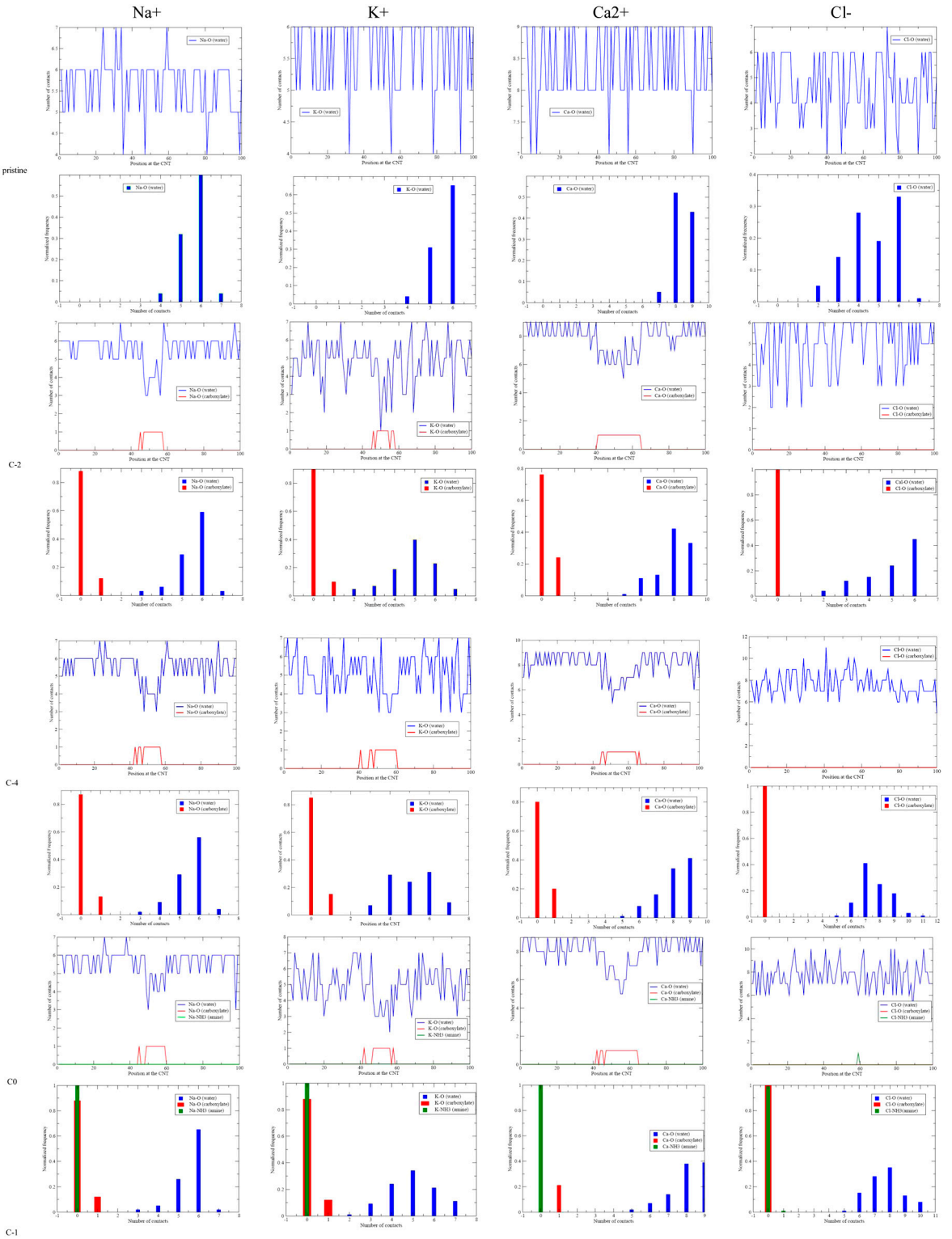

Fig. S6. Coordination of ions inside the CNT in the PMF calculations.

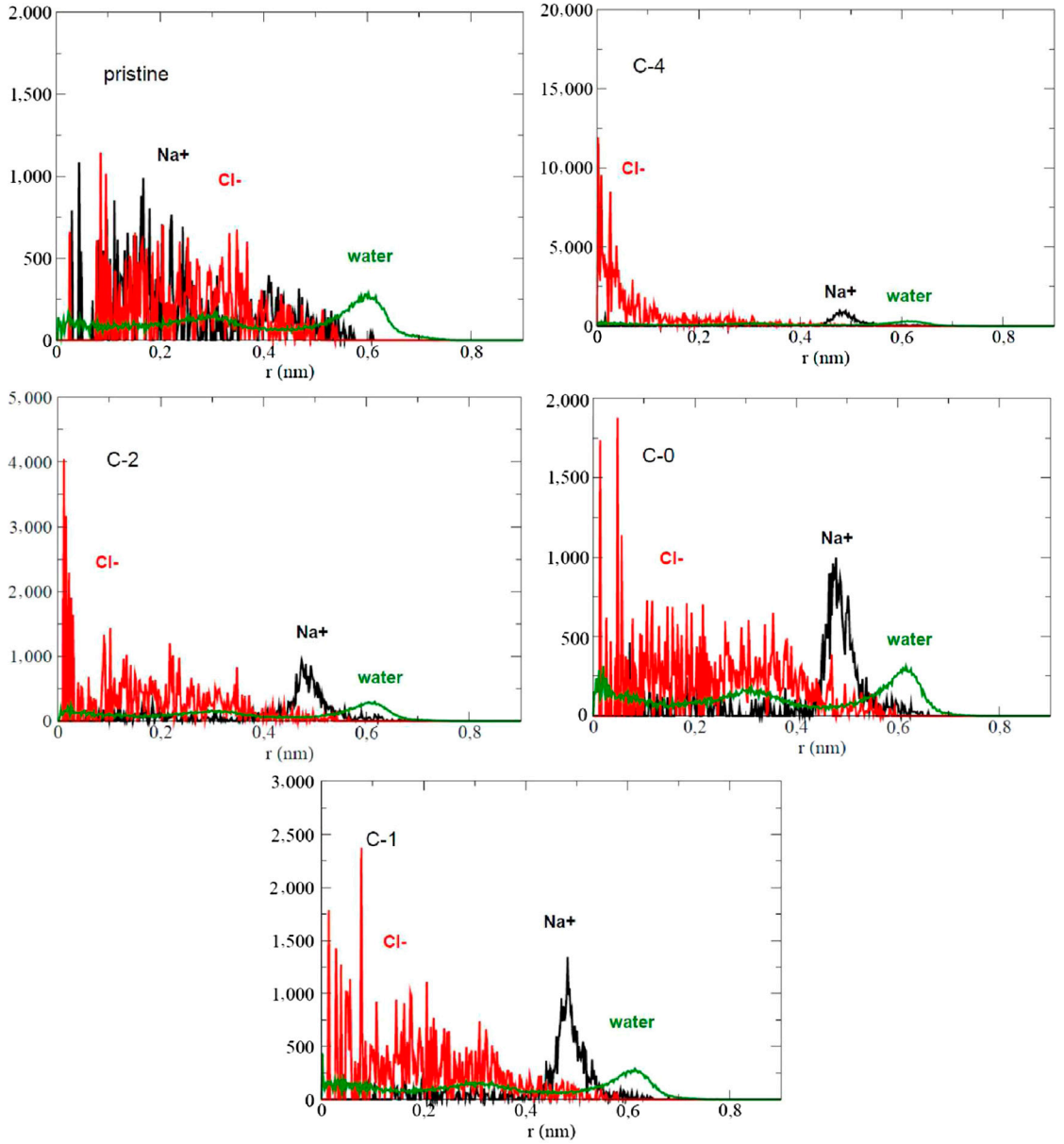

Fig. S7. Radial distributions of Na^+ ions (black), Cl^- ions (red), and water (green) for ions and water inside the nanotube in the vicinity of the selectivity filter, i.e., $|z| < 0.5$ nm.

Table S1 Average number of ion within the nanopore for each simulation

			Pristine	C-4/E-4	C-2/E-2	C-1/E-1	C0/E0	C-EEEE	C-DEKA
Central filter	NaCl 1 M	Na^+	3.5 (1.2)	8.6 (1.1)	6.2 (1.1)	5.3 (1.4)	5.2 (1.2)	7.0 (1.3)	4.8 (1.1)
		Cl^-	4.1 (1.2)	5.3 (1.1)	4.9 (1.2)	4.8 (1.4)	5.6 (1.2)	3.7 (1.3)	4.4 (1.0)
	KCl 1 M	K^+	4.8 (1.3)	9.8 (1.2)	7.4 (1.3)	6.4 (1.4)	5.6 (1.2)	7.0 (1.1)	5.2 (1.5)
		Cl^-	5.1 (1.3)	6.3 (1.2)	5.7 (1.2)	5.8 (1.4)	6.0 (1.2)	3.3 (1.1)	4.5 (1.5)
	$CaCl_2$ 0.5 M	Ca^{2+}	1.1 (0.77)	4.0 (0.6)	3.03 (0.66)	2.9 (0.53)	1.8 (0.67)	3.2 (0.72)	2.3 (0.7)
		Cl^-	2.9 (1.4)	4.3 (0.98)	4.5 (1.2)	5.6 (1.1)	4.2 (1.1)	2.9 (1.2)	4.1 (1.1)
End filter	NaCl 1 M	Na^+	*Same as above*	8.4 (1.3)	6.2(1.3)	5.9 (1.1)	4.8 (1.5)		
		Cl^-		5.3 (1.2)	4.6 (1.4)	5.0 (1.1)	4.7 (1.4)		
	KCl 1 M	K^+		8.4 (1.5)	7.2 (1.3)	6.3 (1.3)	6.2 (1.4)		
		Cl^-		5.2 (1.4)	5.7 (1.3)	5.5 (1.4)	6.2 (1.4)		
	$CaCl_2$ 0.5 M	Ca^{2+}		3.9 (0.52)	3.2 (0.62)	2.4 (0.66)	3.3 (0.75)		
		Cl^-		3.7 (0.99)	4.4 (1.3)	3.3 (1.3)	5.6 (1.5)		

Standard deviations are given in parentheses.

Table S2 Ion diffusion coefficients for selected simulations

	Pristine	C-2	C-4	C-0	C-1
Na^+	0.52 (±0.81)	0.40 (±0.65)	0.23 (±0.60)	0.47 (±0.77	0.24 (±0.51)
Cl^-	0.56 (±0.86)	0.59 (±1.06	0.34 (±0.70)	0.76 (±1.02)	0.38 (±0.47)
K^+	0.60 (±0.89)	0.39 (±0.74)	0.36 (±0.53)	0.29 (±0.50)	0.51 (±0.94)
Cl^-	0.29 (±0.55)	0.58 (±0.96)	0.37 (±0.71)	0.44 (±0.85)	0.53 (±0.86)
Ca^{2+}	0.13 (±0.41)	0.014 (±0.053)	0.013 (±0.0.022)	0.0083 (±0.038)	0.011 (±0.0084)
Cl^-	0.39 (±0.79)	0.73 (±0.95)	0.44 (±0.77)	0.56 (±0.97)	0.53 (±0.77)

The diffusion coefficients (D in units of 10^{-9} m^2/s) are given parallel to the nanopore axis (with standard deviations in parentheses). For comparison, values for diffusion in bulk solution are Na^+ 1.2, Cl^- 1.8, K^+ 1.8, and Ca^{2+} 0.53×10^{-9} m^2/s (1).

1. Koneshan S, Rasaiah JC, Lynden-Bell RM, Lee SH (1998) Solvent structure, dynamics, and ion mobility in aqueous solutions at 25 °C. *J Phys Chem B* 102:4193–4204.